

A High-Bandwidth End-Effector With Active Force Control for Robotic Polishing

JIAN LI¹, YISHENG GUAN¹, (Member, IEEE), HAOWEN CHEN¹, BING WANG¹,
TAO ZHANG¹, (Member, IEEE), XINENG LIU¹, JIE HONG², DANWEI WANG³, (Senior Member, IEEE),
AND HONG ZHANG^{1,4}, (Fellow, IEEE)

¹The Biomimetic and Intelligent Robotics Lab (BIRL), School of Electromechanical Engineering, Guangdong University of Technology, Guangzhou 510006, China

²College of Engineering and Computer Science, The Australian National University, Canberra, ACT 2601, Australia

³School of Electrical and Electronics Engineering, Nanyang Technological University, Singapore 639798

⁴Department of Computing Science, University of Alberta, Edmonton, AB T6G 2E8, Canada

Corresponding authors: Yisheng Guan (ysguan@gdut.edu.cn) and Tao Zhang (tzhang@gdut.edu.cn)

The work in this paper was supported in part by the NSFC-Guangdong Joint Fund (Grant No. U1401240), the NSFC Project for Young Scientists (Grant No. 51905105), the Program of Foshan Innovation Team of Science and Technology (Grant No. 2015IT100072), and the Frontier and Key Technology Innovation Special Funds of Guangdong Province (Grant No. 2017B050506008 and 2019B090915001).

ABSTRACT To promote operational intelligence, improve surface quality, and reduce manpower dependence, a novel high-bandwidth end-effector with active force control for robotic polishing was proposed. Using this end-effector as a mini robot, a macro-mini robot for polishing processing was constructed, in which the macro robot provides posture control during polishing operations, whereas the mini-robot provides constant force control. By minimizing the inertia along the spindle in this configuration, the end-effector obtains a force control bandwidth of 200 Hz. Through a series of comparative experiments with different contact forces and feed rates, the proposed design was proven to have a smaller overshoot, a faster response, and a shorter settling time than the conventional method based on macro robot (KUKA iiwa) controlled force. The roughness of the workpiece reached $0.4 \mu\text{m}$ after polishing with the macro-mini robot, indicating the efficiency of this end-effector in high-precision material removal and surface polishing operations.

INDEX TERMS Robotic polishing, force control, high-bandwidth, macro-mini robot, end-effector.

I. INTRODUCTION

A. CONTEXT

Polishing is widely used to reduce surface roughness and improve machining precision of workpieces in manufacturing processes, such as die, airfoil, camshaft, crankshaft, and sculptures [1]. To date, most polishing operations are still carried out manually, resulting in low efficiency of manufacturing, an inconsistent surface quality of workpieces, and health problem among workers [2]. This is inconsistent with the global trends of Industry 4.0 and restricts the development of industrial manufacturing in the pursuit of intelligence [3], [4].

To solve the low surface quality and manpower shortages of manual polishing, automatic polishing processes represented by computer numerically controlled (CNC) machines

and industrial robots have become the primary solutions. CNC machines not only offer excellent stiffness and remarkable positioning accuracy but can also effectively control the trajectory, posture, and force simultaneously during polishing processes [5]. However, the wide employment of such machines is limited due to their narrow workspaces, the difficulty in clamping complex parts, low system flexibility, and high prices [6]. Compared with CNC machines, industrial robots have the advantages of a lower cost, higher flexibility, and greater integrative capabilities with various end-effectors and sensors. These advantages make industrial robots an effective and economical solution to the process of complex surface material removal, regardless of the workpiece size [7].

In the polishing process, numerous factors affect the final surface quality, such as abrasive topology, tool wear, tool path, contact force, feed rate, and rotational speed [8]. Among these factors, the contact force is a critical factor determining the thermal effect, chip thickness, and final surface roughness

The associate editor coordinating the review of this manuscript and approving it for publication was Yingxiang Liu¹.

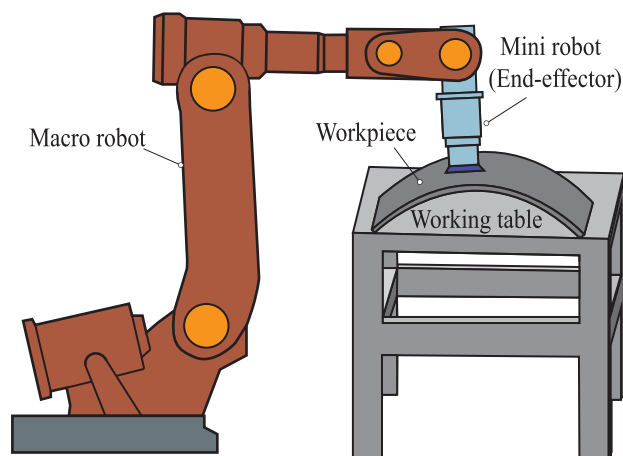


FIGURE 1. Typical macro-mini configuration for robotic polishing.

during polishing operations [9]. Therefore, numerous researchers have verified that the contact force between the polishing tool and the workpiece is the key factor determining polishing quality and efficiency [10]–[13]. According to different processing requirements and conditions, a robotic polishing system is required to follow highly variable contact forces with rapid response and high precision to avoid workpiece surface damage caused by over- or under-polishing [14]. To realize contact force control in robotic polishing, Whitney [15] proposed two primary methods: passive compliance control and active compliance control. As Xie *et al.* [16] proposed, although passive compliance control is relatively simple to implement (it does not need an actuator) and has the outstanding characteristic of a low price, it can only maintain low-precision contact force in short ranges. Obviously, this method is not suitable for high-precision polishing operations. Active compliance control, the main research trend in the robotic force control field [17], can be divided into two categories: through-the-arm systems and around-the-arm systems. A through-the-arm system tracks the desired force by adjusting the whole robot's posture, but its high inertia inevitably leads to a slow response for force control [6]. To improve the force tracking accuracy of this method, Loris Roveda proposed an on-line estimation of the interactive environment stiffness between the robot and the workpiece [18] and a discrete-time formulation for impedance controlled tasks [19] to overcome the force overshoot issue. Whereas an around-the-arm system forms a macro-mini robotic system (Fig. 1) featuring an end-effector with active force control, which decouples posture control and force control during the operational process. Hence, this macro-mini robotic system can increase the force control bandwidth and then obtain rapid dynamic response performance [20].

B. STATE OF THE ART

In the past years, many researchers have focused on improving the hardware design and control strategies for macro-mini

robotic systems. Bone and Elbestawi [21] developed an active compliant end-effector with a DC servo motor and a linear ball screw, which achieved an accuracy greater than 0.01 mm but a control bandwidth of only 20 Hz. Lew [22] proposed a mini robot to achieve a desired contact force, which smoothed the transition of the mini robot from a free-space in an unknown environment. Tol *et al.* [23] integrated an extendable strut type parallel kinematic mechanism and a mini robot into a macro-mini robot and obtained superb performance for low-cost and high-precision deburring operations. Liao *et al.* [24] proposed a compliance mini robot using three pneumatic actuators, whereas the force control performance was limited by the instability and slow response of the pneumatic actuators. Arifin *et al.* [25] introduced a control framework for a macro-mini robot to enhance compliant force control performance, thereby reducing the impact when the mini robot contacts the workpieces. Wu *et al.* [26] proposed an adaptive neural network control compensator for a macro-mini robot to estimate and eliminate the coupling dynamics in real time. Ma *et al.* [20] established a 3-DOF parallel end-effector with complex configuration in a macro-mini robot and obtained a position control bandwidth near 100 Hz. However, Lopes and Almeida [27] indicated that the bandwidth is one-tenth lower in force control than in position control. Mohammad *et al.* [6] proposed a mini robot for polishing process by reducing the inertia along the spindle. However, information on bandwidth and polishing quality was not provided. Chen *et al.* [28] developed a mini robot for polishing thin-walled blisks, which contains complex components such as a positioning table and eddy current damper. Wu *et al.* [29] proposed a force-controlled spherical polishing tool combined with self-rotation and co-rotation motion for an automatic polishing process, which obtained a bandwidth frequency of 900 rad/s. Yang *et al.* [30] designed a three degree-of-freedom (DOF) (i.e., two-rotational and one-translational (2R1T)) end-effector to perform continuous contact operations, which achieved a force control bandwidth of 15 Hz.

C. PAPER CONTRIBUTION

Although the aforementioned researchers have studied various aspects of the macro-mini robotic system (e.g., control strategies, configuration designs, and the addition of auxiliary structures like damping), the force control bandwidth in polishing applications can still be improved. A reasonable method to improve the bandwidth of force control is decoupling control between the position and force through a mini robot with an active force control [6], [20]. The main contributions of this article are as follows:

- 1) Based on investigating the current situation of contact force control in the robotic polishing field, we propose a method to increase the force control bandwidth by reducing the moving inertia. The polishing operation's characteristics conformed to the five design philosophies for an end-effector as shown below.

- 2) Using a force motor that directly drives the polishing head without passing other parts (e.g., the polishing motor, spindle, and force sensor), we propose a novel end-effector with active force control for robotic polishing, which minimizes the inertia along the normal direction of contact.
- 3) Through frequency domain analysis and force control experiments of the proposed end-effector, we obtained the state-of-the-art theoretical and actual force control bandwidth known by authors in the field of robotic polishing.
- 4) Through a series of force tracking and polishing experiments between the proposed end-effector and the macro robot (i.e., a KUKA iiwa robot with excellent embedded force control), the force tracking accuracy and the surface roughness obtained by the proposed end-effector are shown to be better than the results obtained by the macro robot. This verifies the feasibility and rationality of the proposed design in polishing applications.

The remainder of this article is organized as follows: Section II introduces the design philosophy, overall configuration, and key structural analysis of the proposed design. The hardware implementations and control method are presented in Section III. Discussion of the control bandwidth and the experimental results are given in Section IV. Finally, Section V concludes this work and introduces the plans for future work.

II. MECHANICAL DESIGN

A. DESIGN PHILOSOPHY

Considering the diversity, complexity, and importance of contact force control in the polishing process, the design of an end-effector with excellent performance needs to match the following criteria:

- 1) *Individual actuation to decouple movements*: One principle to realize high-precision active force control is to decouple the telescopic movement along the spindle from the rotation around the spindle. Then the contact force can be individually controlled through this configuration. Therefore, it is necessary to decouple these two motions in mechanism design.
- 2) *Low translational inertia to accelerate the response*: In the process of polishing force control, each component superimposed onto the telescopic movement increases the inertial mass and reduces the bandwidth of the dynamic response. For this reason, the translational inertia of the end-effector should be minimized to acquire a fast response for force control.
- 3) *Lightweight parts to decrease mass*: From the viewpoint of system integration, the heavier the end-effector is, the larger the load capability that the macro robot needs to provide, which inevitably increases the cost of the macro robot. Therefore, lightweight optimization should be seriously considered in end-effector design.
- 4) *Optimized connector to increase stability*: The connection style between the end-effector and the macro robot largely determines the system's stiffness and thus influences control stability. To obtain a high-performance macro-mini robotic system, the connection method needs to be considered in the configuration design.
- 5) *Modular design for fast replacement*: To meet the polishing requirements for various workpieces, diverse operation scenarios and macro robots are needed. Modular design of the end-effector could form an independent and universal component that can be easily integrated with different robots or flexibly applied to workpieces with various shapes.

Based on the aforementioned design philosophy, to design an end-effector without compromising performance, an improved configuration was proposed, as shown in Fig. 2. The most important feature of the proposed configuration is that an active force motor directly drives the polishing head to track the desired force (Fig. 2(a)). In a conventional configuration, however, besides the polishing head, the motor also needs to drive many other parts during telescopic movement, such as the polishing motor, spindle, and force sensor (Fig. 2(b)) [6]. In this novel configuration, the moving inertia along the spindle is reduced to the lowest level, thereby offering excellent control bandwidth. In addition, shortening the distance between the macro robot's flange and the polishing head helps to improve the stability of the polishing process [31].

B. END-EFFECTOR CONFIGURATION

A sectional view of the proposed configuration is shown in Fig. 3, which consists of three components: a rotational component, a telescopic component, and a macro-mini connector.

- 1) **Rotational component**: The rotational movement originating from the polishing motor (1) is transmitted to the spline nut (17) through the polishing spindle (3). The spline nut (17) drives the polishing head (16) to rotate, thereby realizing the movement of the polishing pad (18). During the transfer of rotational motion, there is no redundant intermediate transmission part besides the necessary polishing spindle (3), which greatly reduces energy loss and increases structural compactness. In this configuration, the combination of the spline nut (17) and bearing III (15) is the key to decoupling the rotational and telescopic motions of the polishing head (16). To reduce the impact of the longer spindle and improve the configuration's stability and stiffness, bearings I (4) and II (8) are used to limit the axial and radial movements of the spindle (3), respectively. The polishing pad (18) is designed as a modular part to make it easier to handle various complex workpieces and polishing paths by changing its size. A pneumatic motor was selected as the polishing motor because it weighs only one-third of a servo motor with the same power. The whole mass of this end-effector

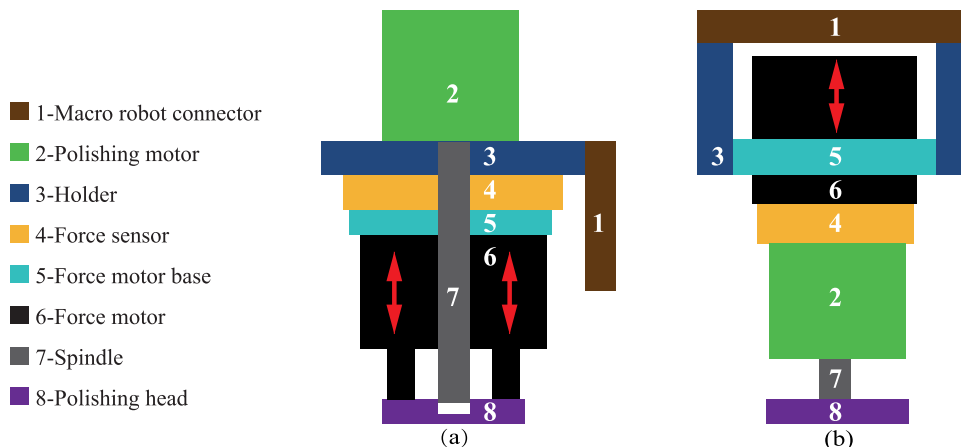


FIGURE 2. Proposed configuration versus conventional configuration. (a) The proposed configuration minimizes the inertia along the spindle, reduces the middle connection for force transfer, and adopts a L-type connector to shorten the distance between the macro robot’s flange and polishing head. (b) The conventional configuration, whose force transfer needs to pass through multiple middleware sections with a relatively large inertia, and connect with the macro robot’s flange at the top, resulting in a relatively larger distance and reducing system stiffness.

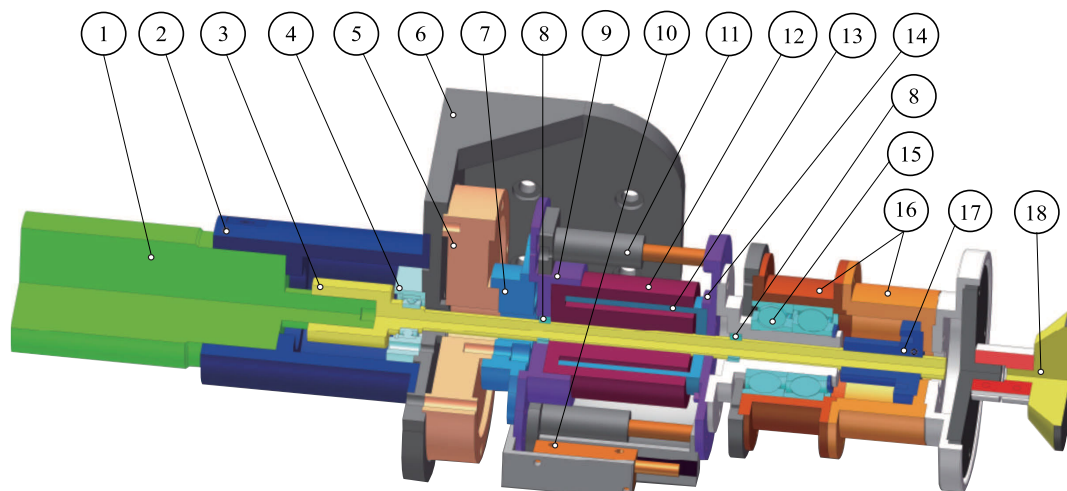


FIGURE 3. Configuration details of the proposed end-effector. Part names in the picture: 1-Polishing motor, 2-Motor bracket, 3-Spindle, 4-Bearing I, 5-Force sensor, 6-L-type connector, 7-Connector I, 8-Bearing II, 9-HVCM housing, 10-Sliding rod, 11-Linear encoder, 12-HVCM magnetic housing, 13-HVCM Coil, 14-Connector II, 15-Bearing III, 16-Polishing head, 17-Spline nut, and 18-Polishing pad.

is 5.12 kg, which is far less than that of conventional end-effectors with active force control in the polishing filed. Thus, this end-effector can be connected to most industrial robots’ flanges.

- 2) **Telescopic component:** To construct a closed-loop force control system and minimize the axial inertia, a linear hollow voice coil motor (HVCM) is utilized for active force control. The HVCM housing (9) is connected to the force sensor (5), which is fixed to the framework (*L*-type connector (6)) through connector I (7), and the coil (13) is connected to the polishing head (16) through connector II (14). The inertia along the spindle is minimized by this method. Notably, the active part of the HVCM is the coil (13) that moves along a straight line relative to the magnetic hous-

ing (12), realizing telescopic motion along the polishing spindle (3) to provide the contact force towards workpieces. To ensure structural rigidity and minimize operational vibrations, the coil (13) is mounted to connector II (14) with sliding rods (11), and a linear encoder (10) is utilized to ensure the accuracy of the telescopic motion. During the polishing processes, the sensor (5) feeds back the contact force signals in real-time, whereas the HVCM controls the contact force through the coil’s (13) telescopic motion.

- 3) **Macro-mini connector:** The *L*-type connector (6) is designed to keep the polishing motor (1), the polishing spindle (3), the force sensor (5), and other components stationary. Unlike the conventional configuration, by using the *L*-type connector (6), the connection

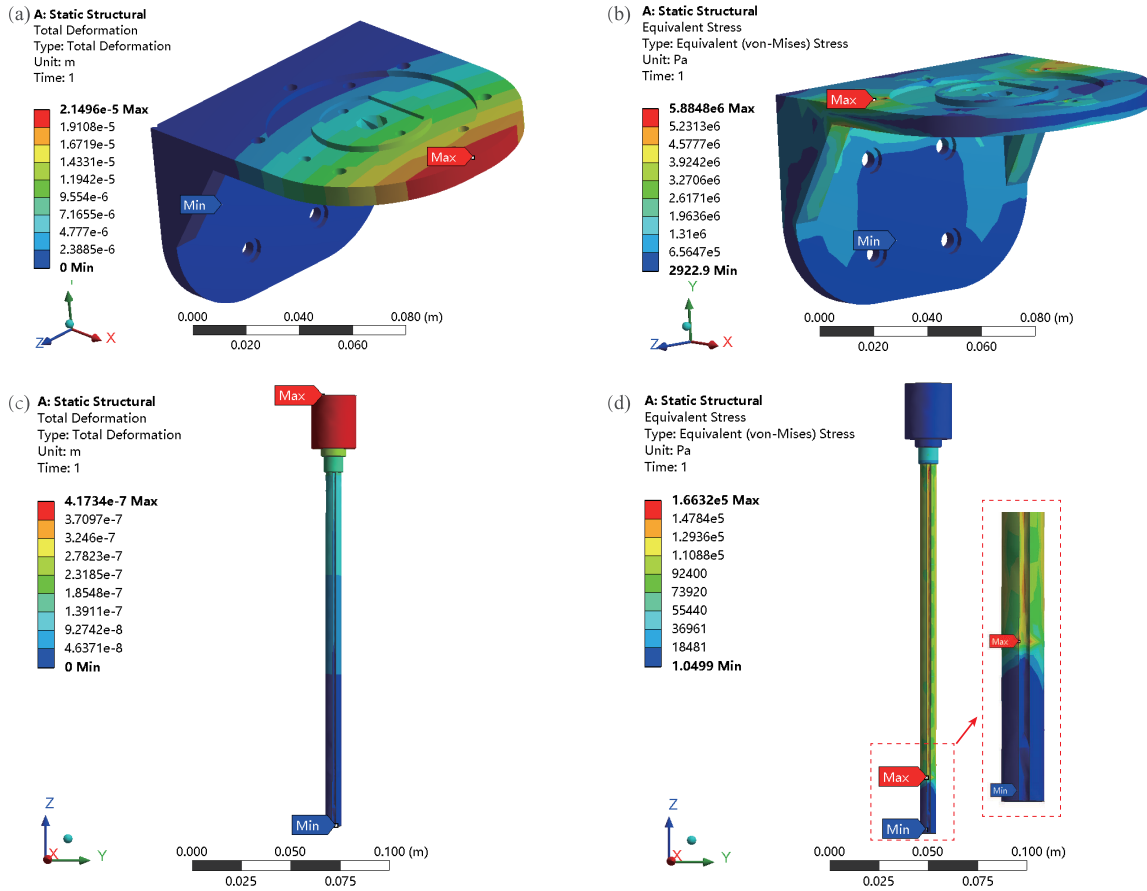


FIGURE 4. FEA results of the key parts of the proposed end-effector. (a) Total deformation result of the L-type connector. (b) Equivalent stress result of the L-type connector. (c) Total deformation result of the spindle. (d) Equivalent stress result of the spindle.

section between the macro robot and the mini robot is moved from the top to the middle of the mini robot. Shortening the distance between the macro robot's flange and the workpiece is conducive to suppressing vibrations and improving stability during the polishing process [31].

Based on the aforementioned design, by utilizing various polishing paths and polishing pads, the proposed end-effector can process workpieces of numerous materials, such as metal, wood, and soft materials, as well as workpieces of diverse surface shapes, such as flat, slope, free-form and complex irregular surfaces.

C. FINITE ELEMENT ANALYSIS

Since the proposed design targets for contact force and cutting torque range up to 50 N and 3.5 Nm during the polishing process, it is necessary to ensure a reliable connection between the macro robot and the mini robot, as well as stable torque transmission from the polishing motor to the polishing pad. Therefore, finite element analysis (FEA) modeling and simulations were employed to analyze the structure of the L-type connector (6) and the spindle (3) using ANSYS Workbench 18.0. As the L-type connector (6) connects the macro robot and the mini robot and carries the full weight of

the mini robot, to analyse the deformation and stress (with C45 steel), the side connected to the macro robot was fixed, and then an 80 N payload (safety factor 1.6) was applied to the upper surface. It can be seen in Fig. 4(a) that the total deformation of the L-type connector is only 21.50 μm, while Fig. 4(b) shows that the equivalent stress is 5.88×10^6 Pa, which is far smaller than the yield stress of C45 steel (3.55×10^8 N/m²). The spindle (3), which transfers the rotation from the polishing motor (1) on the top of the mini robot to the polishing pad (18) on the bottom, was also analyzed to determine its deformation and stress through FEA with the chosen material of Q235 steel. We fixed the bottom section of the spindle contacting the spline nut (17) and employed a torque of 6 N/m (safety factor 1.7) to the shaft sleeve connected to the polishing motor (1); the analysis results are shown in Fig. 4(c-d). It can be seen from Fig. 4(c) that the total deformation of the spindle is only 0.42 μm, while Fig. 4(d) shows that the equivalent stress is 1.66×10^5 Pa, which is far lower than the yield stress of Q235 steel (2.35×10^8 N/m²). From the results shown in Fig. 4, it can be concluded that the stress and deformation of the L-type connector and the spindle are within a safe range, which indicates that the proposed design is reasonable and reliable.

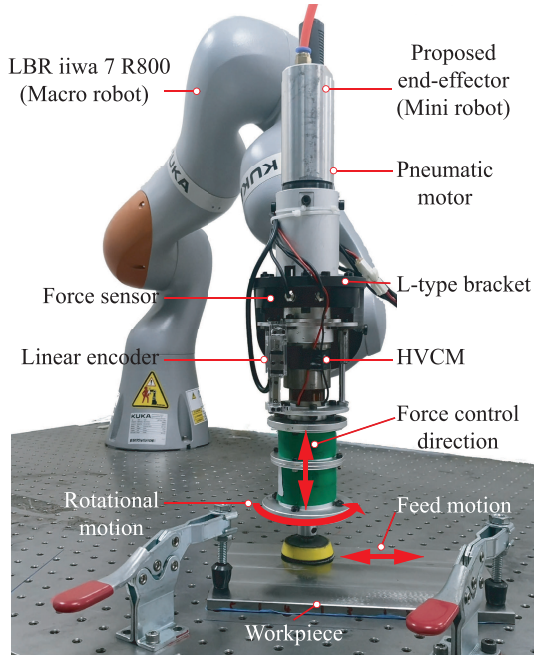


FIGURE 5. Macro-mini robotic polishing platform for experiments.

III. HARDWARE IMPLEMENTATION AND CONTROL METHOD

A. HARDWARE IMPLEMENTATION

A macro-mini robotic polishing platform was established to verify the proposed design, as shown in Fig. 5. A KUKA LBR iiwa 7 R800 robot with excellent force control was employed as the macro robot, controlled by KUKA Sunrise OS running on KUKA Sunrise Cabinet control hardware. The weight of the proposed design (5.12 kg) is within the payload (7 kg) limits of the KUKA iiwa, and the weight of the telescopic part (2 kg) of the end-effector is supported by the workpiece during the contact operation, reducing the payload of the KUKA iiwa. Therefore, the weight of the proposed device will not affect the performance of the KUKA iiwa. Moreover, the KUKA iiwa used in this article has two independent position and impedance (force) control modes. When the position control mode is adopted, the force control mode is ineffectiveness, and vice versa. These characteristics make the KUKA iiwa a good counterpoint to verify the performance of the proposed design.

The mini robot includes a pneumatic motor (model JC-260) as the polishing motor, which has a power of 640 W, a torque up to 3.9 Nm, and a rated rotational speed up to 2100 rpm. The polishing pad utilized for the experiments has a diameter of 25 mm. An HVCM (model TMEC0070-015-000) with a 27.9 N continuous output force (peak force up to 70 N) and a 15 mm stroke was employed as the force motor. The HVCM was run in the current control mode with a force amplifier gain (K_m) of 17.7 N/A. Once the coil was energized, contact force was generated between the polishing pad and the workpiece. Then, the contact force in the normal direction (as shown in Fig. 5) was measured by a force sensor (model

LH-LN-01 with a sampling rate of 2.5 kHz) and fed back to the control platform (i.e., MATLAB R2019a under Windows 10 OS in this study) through a voltage amplifier (model 170LH-FD-S) and a data acquisition card (model USB-231). After being processed by the control platform, the control signal was sent to a Copley controller (model ACJ-055-18 with a sampling rate of 1.3 kHz) to drive the HVCM and thus realize the closed-loop force control. The integrated hardware platform for validating the force control performance of the end-effector is shown in Fig. 6.

B. CONTROL METHOD

Under the current mode, the output telescopic force of the HVCM F_m is proportional to the input current i , i.e., $F_m = K_m i$. Considering the gravity of the polishing head, the contact force F_c is the sum of the motor force F_m and the preload F_p provided by the polishing head (i.e., $F_c = F_m + F_p$) and is measured and fed back by the force sensor. Assuming the desired contact force is F_d , the force tracking error F_e between the measured force and the desired contact force can be expressed as:

$$F_e = F_d - F_c = F_d - K_m i - F_p \quad (1)$$

To eliminate F_e , a closed-loop force control was constructed through the PID control algorithm, and the force control scheme is shown in Fig. 7. The feedback signal u_f is shown below:

$$u_f = (F_d - F_p + K_p F_e + K_i \int_0^t F_e dt + K_d \frac{dF_e}{dt}) / K_m \quad (2)$$

where K_p , K_i and K_d are the proportional, integral and derivative gains of the PID algorithm, respectively. By choosing suitable K_p , K_i and K_d values, Eq. (2) is asymptotically stable, while Eq. (1) tends to be zero; in this way, the desired contact force F_d can be reached. To eliminate high-frequency noise during polishing, a low-pass filter was employed to process the feedback force signals. The electromechanical model of the end-effector during polishing processes is shown in Fig. 8, and the transfer function between the telescopic motion and the control signal can be expressed as:

$$\frac{X(s)}{U(s)} = \frac{K_m}{Lms^3 + (Lc + Rm)s^2 + (Rc + K_m^2)s} \quad (3)$$

As the stator inductance L is very small, its impact can be neglected [32]. Hence, Eq. (3) can be described by the following dominant second-order transfer function:

$$\frac{X(s)}{U(s)} = \frac{K_m}{Rms^2 + (Rc + K_m^2)s} \quad (4)$$

Eq. (4) is the system's open-loop transfer function. Hence, by integrating the PID controller $G_c(s) = (K_d s^2 + K_p s + K_i) / s$ and the force $F(s) = K_{stiff} X(s)$, the closed-loop transfer function for the end-effector's force control can be expressed as Eq. (5), as shown at the top of the next page, where $F_d(s)$ is the Laplace transformation of F_d , and K_{stiff} is the equivalent stiffness of workpiece.

$$\frac{F(s)}{F_d(s)} = \frac{K_m K_{stiff} K_d s^2 + K_m K_{stiff} K_p s + K_m K_{stiff} K_i}{R m s^3 + (R c + K_m^2 + K_m K_{stiff} K_d) s^2 + K_m K_{stiff} K_p s + K_m K_{stiff} K_i} \quad (5)$$

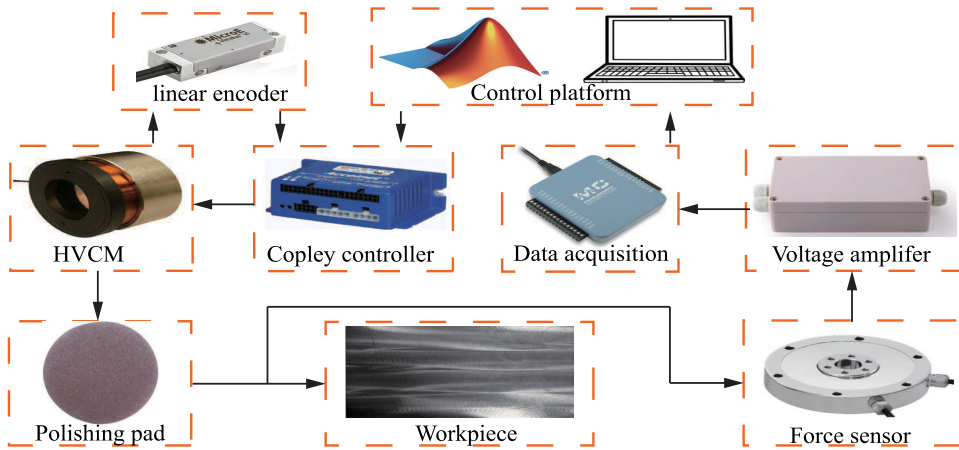


FIGURE 6. Hardware platform for force control performance validation.

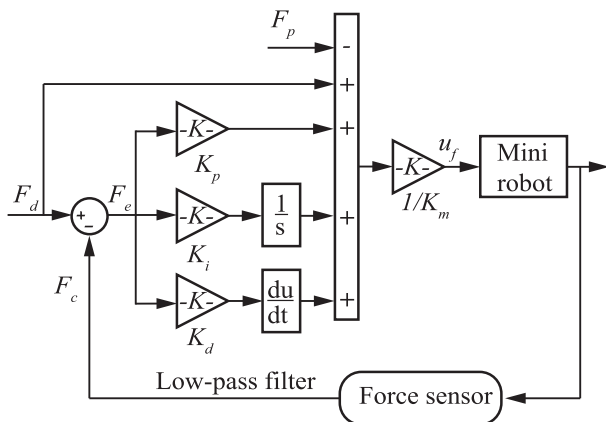


FIGURE 7. Scheme of the proposed force control system.

IV. SYSTEM PERFORMANCE VALIDATION

A. DYNAMIC RESPONSE PERFORMANCE

During polishing processes, the macro-mini robotic system needs to maintain the desired contact force. Especially with highly variable or non-uniform surfaces, the system needs to adjust its contact force with a fast response to avoid over- or under-polishing.

The frequency response spectrum is a good method to evaluate the dynamic response performance (DRP) of the end-effector [20]. It is generally known that the DRP of an actual system is influenced by many factors, such as PC performance, the programming mode, the software platform, hardware transmission, and signal processing. To better analyze the DRP of the proposed design without losing generality, we only considered the response of the end-effector and neglected all the factors related to signal transmission and processing. The key parameters were put into MATLAB for calculations. According to the force tracking effect

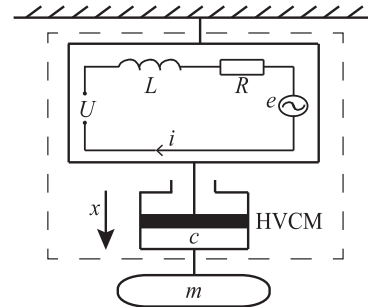


FIGURE 8. Electromechanical model of the end-effector. U -total voltage of the coil, L -stator inductance coefficient, R -resistance coefficient, e -counter electromotive force, i -motor current, x -motor position, c -damping coefficient, and m -total mass of all moving parts.

corresponding to various K_p , K_i and K_d parameters in a simulation model of the proposed end-effector force tracking constructed based on Simulink, K_p , K_i and K_d were selected as 4000, 20, and 0.01, respectively. Substituting these three parameters with $K_m = 17.7$, $R = 6.8$, $c = 0.2$, $m = 2$ and $K_{stiff} = 200$ (the value of common steels elastic modulus) into the closed-loop transfer function Eq. (5), the theoretical bandwidth of the end-effector was obtained (Fig. 9(a)) based on the Bode function in MATLAB R2019a.

From Fig. 9(a), it can be seen that the frequency response of the proposed end-effector was attenuated to -3 dB with a theoretical bandwidth of 1510 rad/s, which is a significant increase of 67.77% from the theoretical bandwidth of 900 rad/s obtained in a recent robotic polishing theoretical analysis [29]. When using the whole system shown in Fig. 6 to perform force tracking experiments under different control periods (20-2000 Hz), it was found that the shortest settling time of the target force can be obtained at a bandwidth of 200 Hz, as shown in Fig. 9(b). As mentioned above, because the actual force control experiment inevitably has a

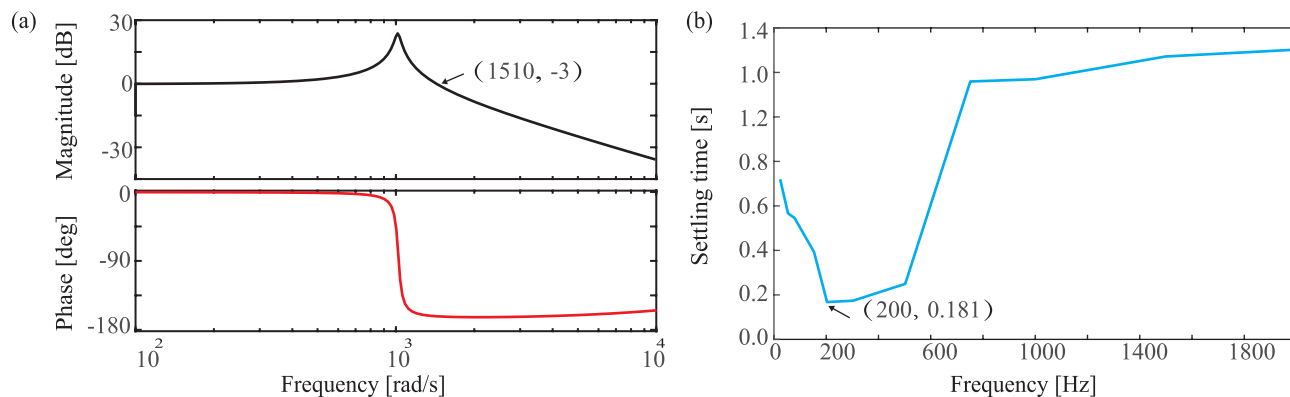


FIGURE 9. Bandwidth of the proposed end-effector. (a) Theoretical bandwidth of the frequency characteristic Bode diagram; (b) Actual bandwidth of the force control experiments.

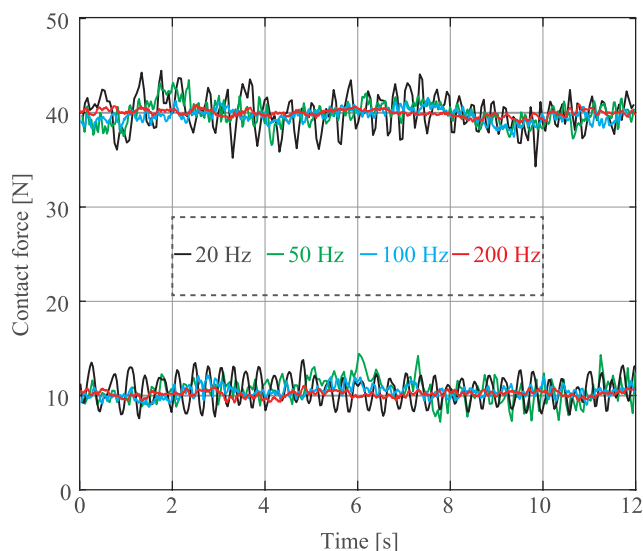


FIGURE 10. Force tracking results under different control bandwidths.

delay, the actual bandwidth of 200 Hz is slightly smaller than the theoretical value of 240 Hz (i.e., 1510 rad/s). However, compared to the actual control bandwidth of 100 Hz obtained in the recent robotic polishing research [20], the bandwidth obtained in our proposed design has a significant improvement of 100%. This is coincident with the proposed design philosophy, which involves achieving a high bandwidth by minimizing the moving parts related to the contact force control. Exhausting the author’s knowledge, this design provides the state-of-the-art bandwidth in the field of robotic polishing. Such a high bandwidth can satisfy most polishing applications requiring high-speed dynamic responses.

To test the suppression effect of the high-speed dynamic response produced by the high bandwidth of the force vibration caused by unknown interference factors during the force control process, we employed 20 Hz, 50 Hz, 100 Hz, and 200 Hz control bandwidths to perform force tracking experiments at 10 N and 40 N, as shown in Fig. 10. Notably, to ensure a fair comparison, the changed parameter in each

experiment was only the control bandwidth. It can be clearly seen in Fig. 10 that regardless of the level of contact force, as the control bandwidth increases, the tracking accuracy is also improved accordingly. This also means that a control scheme with high bandwidth can suppress the noise generated during force control.

B. FORCE CONTROL PERFORMANCE

The contact force is a critical parameter influencing polishing quality and efficiency, which should be adjusted according to the polishing process with a rapid response and a minimized overshoot [33].

To further validate the proposed design, this article designed force tracking experiments under different contact forces and feed rates. In these experiments, the macro robot carried the mini robot to contact a flat stainless steel workpiece (240 × 120 × 8 mm), and horizontally polished along the long side of the workpiece through a polishing pad (25 mm diameter) with a 240 grit size sandpaper. Notably, since the situation during the actual force control process is more complicated than in the above simulation, to make the proposed design work efficiently, we have re-selected the PID parameters in the following experiments as follows: $K_p = 0.15$, $K_i = 5$ and $K_d = 0.01$. In addition, a 5th-order Butterworth low-pass filter with a cut-off frequency of 10 Hz was used to suppress the high-frequency noise in all control loops. Moreover, according to the analysis results in the above subsection, to make the proposed design work in an optimal state, the control bandwidth of all subsequent force control experiments was 200 Hz.

To ensure that results of the force control experiments were not affected by the workpiece surface’s topography, the steel plate used in this article was pre-processed via milling, as shown in Fig. 11. Due to the characteristics of milling, machining marks will inevitably be left on the workpiece surface, such as the slashes shown in Fig. 11(a-b), which were obtained with the Olympus LEXT OLS4000 under 10 times magnification. These slashes were used to verify the effect of subsequent polishing experiments. Then,

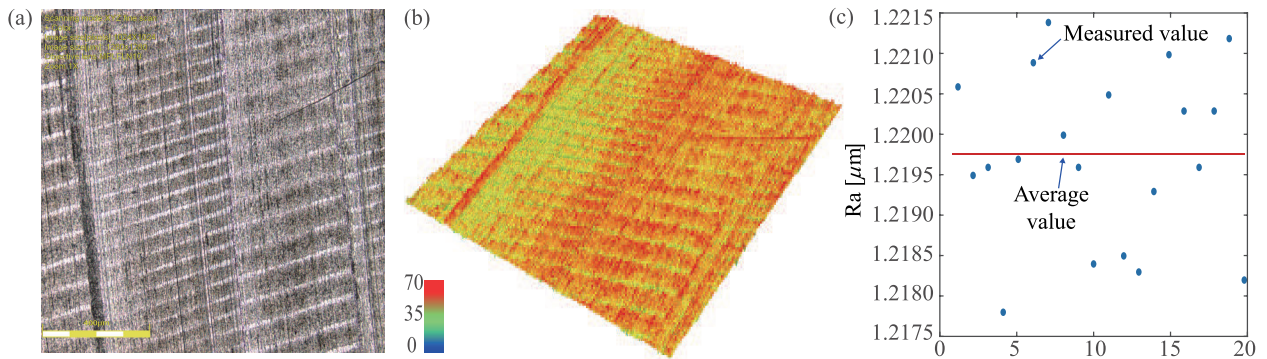


FIGURE 11. Workpiece surface after milling without polishing. (a) 2D topography of the workpiece surface after milling (before polishing), with a scale bar of 400 μm . (b) The corresponding 3D topography of (a), where the colored scale bar (unit μm) denotes the height of the workpiece surface. (c) Roughness measurement values of 20 selected areas on the entire surface of the workpiece.

we divided the milled workpiece into 20 areas and measured the surface roughness of each area with Mahr XT-R 20. The measurement results are shown in Fig. 11(c). It can be seen that the measurement results are in a narrow range around 1.2178 ~ 1.2214 μm . This can be considered a consistent surface with a surface roughness of 1.2197 μm (the average of 20 surface roughness values), which is the baseline for evaluating the surface roughness of the workpiece after polishing.

1) LOW-HIGH FORCE TRACKING TEST

To better determine the performance of this design, a group of contrastive tests were conducted, in which the contact force was controlled using a macro robot (i.e., KUKA iiwa) with excellent force control performance. To ensure a fair comparison, when the macro robot performed force tracking or polishing experiments, the force driving motor (HVCM) of the mini robot was turned off and only provided rotational motion during the polishing process without participating in contact force control. Conversely, when the mini robot performed the force tracking and polishing experiments, the macro robot only provided feed motion and did not participate in the contact force control. For a better comparison, the contact forces of both tests were measured by the force sensor integrated into the mini robot (i.e., part 5 in Fig. 3). To verify the force control performance, the proposed end-effector and the macro robot were required to track two force step signals under the same feed rate of 15 mm/s. The first / second step signal of desired force started at 7 / 37 N, then followed by a rising edge to 15 / 45 N, and reduces back to 7 / 37 N by a falling edge.

First, we validated the force tracking performance without rotational movement, and the results are shown in Fig. 12(a). It can be clearly seen that whether the desired contact force is low or high, compared with the proposed end-effector, the tracking results of the macro robot have a larger overshoot and need a longer stabilization time. Moreover, when the contact force is low, the macro robot reveals a state of performance degradation. These situations occur because the macro robot controls the force via the through-the-arm system, whose large inertia limits the response capability. Therefore, it is

difficult for the macro robot to accurately track the desired force, especially in the case of fine-tuning (low contact force tracking), when vibration and overshoot occur at the same time. Conversely, in the proposed end-effector, the moving inertia is greatly reduced, enabling it to respond faster to compensate for disturbance while retaining strong tracking performance.

When the rotational movement was included in the tests, the polishing motor of the proposed design (i.e., part 1 in Fig. 3) was turned on with a rotational speed of 1100 rpm, which is the continuously and smoothly output rotational speed of the employed pneumatic motor. The force tracking results are shown in Fig. 12(b). The macro robot here shows poor force control performance when the polishing motor is turned on. Especially, when the desired contact force is low, it can hardly follow the value. When tracking high contact force, there is larger overshoot and vibration. Moreover, the tracking curve of the macro robot shows larger overshoot in tracking the falling edge signal. This can be interpreted as the macro robot adopting impedance control to achieve force control. Therefore, the robot needs to move towards the opposite direction to reduce the contact force, which is different from following the rising edge signal. Due to the large inertia of the robotic body, the reverse motion control process is relatively easy to over-adjust, resulting in a larger overshoot in tracking the falling edge than the rising edge. In contrast, the proposed end-effector tracks the desired force with a smaller overshoot and faster response due to the inertial reduction.

We also compared the control currents of HVCM when the polishing motor was turned on or off, as shown in Fig. 12(c). When the rotational polishing movement was excluded, the control current was much gentler, reflecting good control performance. Although the rotational motion has an impact on force tracking, the end-effector still maintains good stability and smoothness in following the desired force.

Employing the Olympus LEXT OLS4000 with 10 times magnification, Fig. 13(a-b) shows the three-dimensional (3D) topographies of the workpiece surface after polishing using

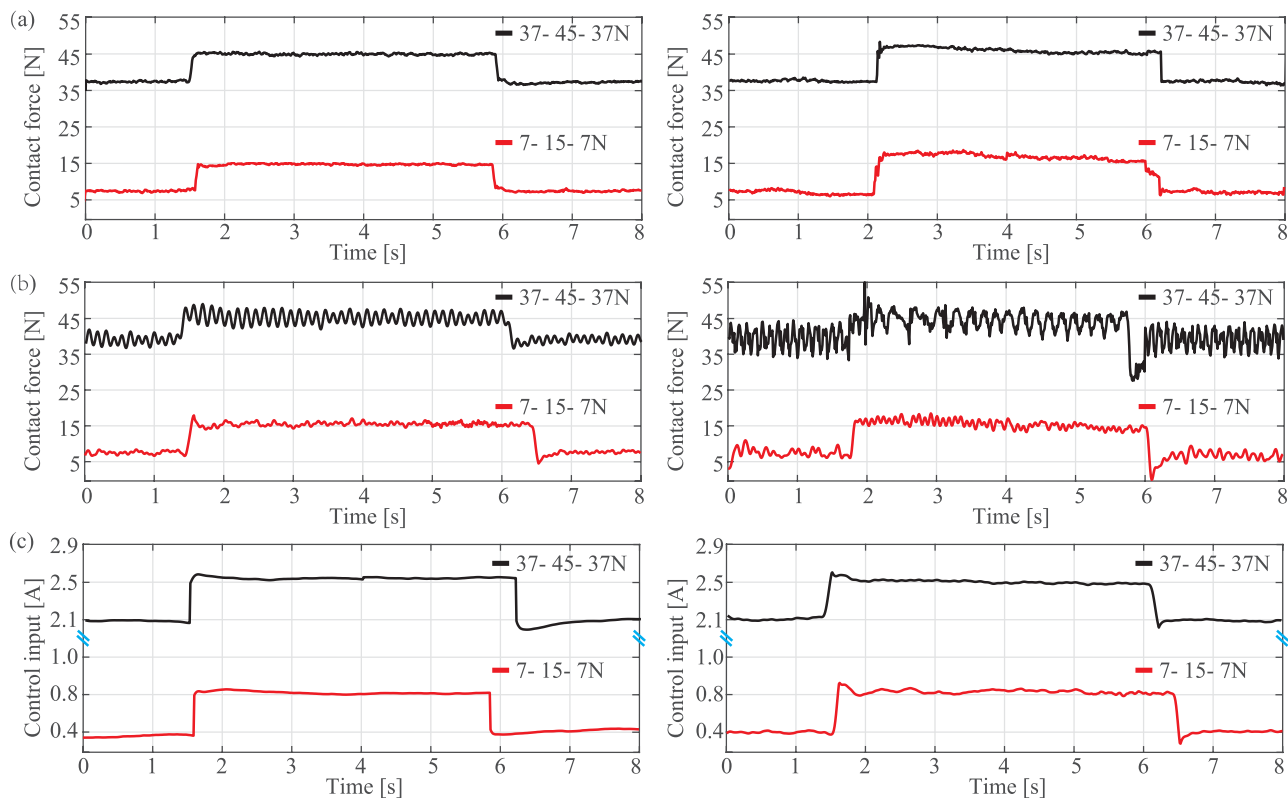


FIGURE 12. Force tracking results under different step signals. (a) With a feed rate of only 15 mm/s: using the proposed end-effector (left) and the macro robot (right). (b) With a feed rate of 15 mm/s and a rotational speed of 1100 rpm: using the proposed end-effector (left) and the macro robot (right). (c) The control current of HVCM under different step signals: using (a)-left without rotational movement (left), and (b)-left with rotational movement (right).

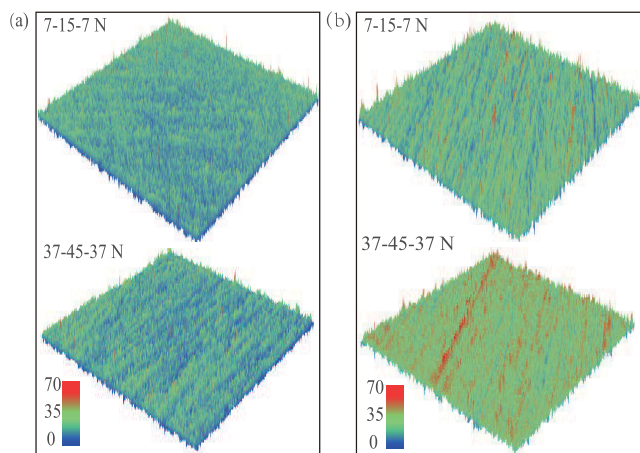


FIGURE 13. 3D topographies of the workpiece surface after polishing; the colored scale bar (unit μm) denotes the height of the workpiece surface. (a) Results of Fig. 12(b)-left. (b) Results of Fig. 12(b)-right. All pictures were obtained by an Olympus LEXT OLS4000 under 10 times magnification.

the proposed end-effector and the macro robot controlling the contact force. Figure 13 demonstrates that both the proposed end-effector and the macro robot can decrease the machining marks from the milling processing shown in Fig. 11(b). Comparing the 3D topographies on the left and right sides of Fig. 13, we observe that when using the macro robot to

track the polishing force with a small value, the workpiece surface shows some remained undulating. When the desired contact force increased, the surface fluctuation became more severe. Therefore, there are still some slashes visible in the 3D topography in Fig. 13(b). The results clearly show that the surface consistency of the workpiece obtained by the proposed end-effector is much better than that obtained by the macro robot regardless of the desired force value, and this is consistent with the results of the force following performance shown in Fig. 12(b).

2) SLOW-FAST FEED RATE TRACKING TEST

Experiments were also carried out to verify the performance of the proposed design in tracking the desired force under different feed rates (i.e., 5 and 30 mm/s). The end-effector and the macro robot were required to track a step force signal starting at 25 N, followed by a rising edge to 35 N, and a reduction back to 25 N with a falling edge.

Similarly, the rotational polishing movement was also excluded in first validation, and the experimental results are shown in Fig. 14(a). With a slow feed rate of 5 mm/s, it can be seen that the macro robot needs a longer settling time to deal with steady-state errors, while the proposed end-effector presents only small overshooting oscillations in the rising and falling edges, as well as a shorter settling time.

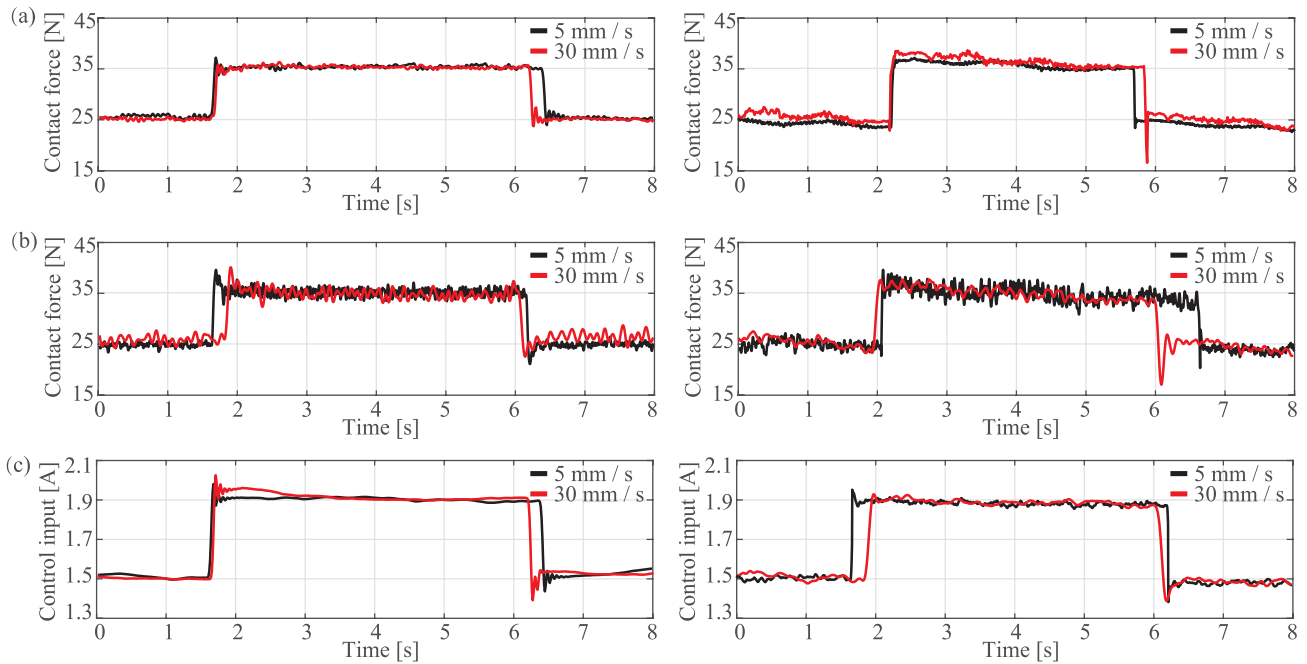


FIGURE 14. Force tracking results under different feed rates. (a) With a 25-35-25 N step signal and without rotational polishing movement: using the proposed end-effector (left), and using the macro robot (right). (b) With a 25-35-25 N step signal under rotational polishing movement (1100 rpm): using the proposed end-effector (left) and using the macro robot (right). (c) The control current of the HVCM under different feed rates with a 25-35-25 N step signal: (a)-left without polishing movement (left), and (b)-left with polishing movement (right).

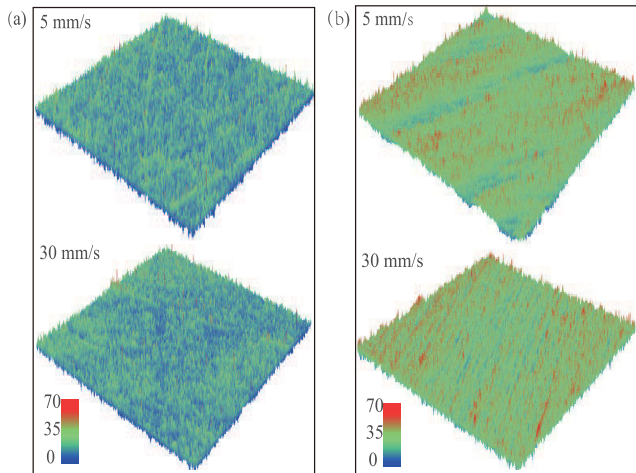


FIGURE 15. Topographies of the workpiece surface. (a) and (b) are the 3D topographies obtained in Fig. 14(b)-left and Fig. 14(b)-right, respectively. The colored scale bar (unit μm) denotes the height of the workpiece surface. All pictures were obtained by an Olympus LEXT OLS4000 under 10 times magnification.

After increasing the feed rate to 30 mm/s, the macro robot shows more severe overshoot, oscillations, and unsteadiness in its force control. Especially in tracking the falling edge, there is a large overshoot, which indicates that an increase in the feed rate aggravates the influence of inertia. In contrast, the proposed end-effector tracks the desired force well, even at a low feed rate.

The experimental results for rotational polishing movement (1100 rpm) under actual polishing condition are presented in Fig. 14(b). As seen in Fig. 14(b), compared to the

macro robot, the proposed end-effector tracks the desired force more accurately with a smaller overshoot and a shorter settling time, regardless of the feed rate.

The HVCM control currents with the polishing movement included or excluded are shown in Fig. 14(c). Similar to the results shown in Fig. 12(c), the control current is much smoother and more stable without the rotational movement because this motion does most of the work in material removal during polishing processing, generating mechanical vibrations and increasing control difficulty.

From the 3D topographies of the polished workpiece surface shown in Fig. 15, it can also be seen that the surface of the workpiece obtained by the proposed end-effector controlling the contact force is smoother and more consistent (Fig. 15(a)). However, the 3D topographies of the workpiece surface after polishing with the macro robot controlling the contact force still retain a few slashes from the milling processing, as shown in Fig. 15(b). We believe this result is related to the poor force control effect shown on the right side of Fig. 14(b).

The surface roughness (measured by Mahr XT-R 20) of the workpiece after five times of repeated polishing experiments is shown in Table 1. The roughness of each experiment is the average value of four measurements using different surface areas. As can be seen in Table 1, the surface roughness obtained by the proposed end-effector is greatly improved over that obtained by the macro robot, which is consistent with the results for the polishing force control in Figs. 12(b) and 14(b), and the 3D topographies in Figs. 13 and 15. Compared to the macro robot, the roughness was improved by 24.70%~34.17% by utilizing the proposed end-effector,

TABLE 1. Polished surface roughness comparison using the proposed end-effector and the macro robot.

Rotational speed rpm	Processing parameters		Time s	Initial roughness before polishing Ra (μm)	Obtained roughness by the proposed end-effector Ra (μm)	Obtained roughness by the macro robot Ra (μm)	Improving ratio %
	Feed rate mm/s	Contact force N					
1100	15	7 - 15 - 7	40	1.2197	0.3498	0.4899	28.60
	15	37 - 45 - 37			0.3977	0.6041	34.17
	5	25 - 35 - 25			0.3557	0.4755	25.19
	30	25 - 35 - 25			0.3868	0.5137	24.70

reflecting the proposed end-effector's efficiency in obtaining better surface quality.

V. CONCLUSION AND FUTURE WORK

To realize intelligent polishing operations and improve the surface quality of a workpiece, robotic polishing is an important and promising method that has been widely used. In polishing processing, the contact force is an important parameter that determines the operational efficiency and final surface quality of a workpiece.

In this article, a novel end-effector with active force control was proposed as a mini robot, and a macro-mini robotic system was constructed to handle the polishing process. Unlike conventional macro-mini robotic polishing systems, the proposed design greatly reduces the inertia along the spindle. Through frequency domain analysis and force control experiments, the proposed system obtains a theoretical bandwidth of 1510 rad/s (i.e., 240 Hz) and an actual bandwidth of 200 Hz, respectively. This represents a significant increase of 67.77% and 100% compared to the theoretical and actual bandwidth of recent research on robotic polishing, respectively. To the authors' knowledge, the proposed design obtained the state-of-the-art bandwidth in the robotic polishing field in terms of dynamic responses in polishing force tracking. Based on a series of contrastive force-tracking experiments between the proposed end-effector and the macro robot, the results when using the proposed end-effector showed a smaller overshoot, a faster response, and a shorter settling time when following the desired force, as well as better surface quality (a surface roughness improvement of 24.70%~34.17%).

Although the proposed end-effector is more convenient in force control than the macro robot, we also found that the tracking effect of the contact force degraded when the rotational movement is included. High bandwidth can indeed achieve better control effects than low bandwidth under the same experimental conditions (as shown in Fig. 10). In different experimental conditions, however, a force control strategy based only on the conventional PID method or the fixed value of the controller parameters has certain limitations, especially in the actual polishing process. Therefore, we plan to investigate the use of methods such as fuzzy adaptive control to achieve more robust force control strategies for dynamic polishing processing and the real-time adjustment of control parameters. Moreover, since the polishing operation is a complicated process, besides the contact force, there are many other factors that can affect the final surface quality,

such as abrasive topology, tool wear, thermal effect, rotational speed, tool path, and feed rate. How these factors influence the final surface quality is also a future research priority.

REFERENCES

- [1] P. Xu, C.-F. Cheung, B. Li, L.-T. Ho, and J.-F. Zhang, "Kinematics analysis of a hybrid manipulator for computer controlled ultra-precision freeform polishing," *Robot. Comput.-Integr. Manuf.*, vol. 44, pp. 44–56, Apr. 2017.
- [2] K. Ma and G. Yang, "Kinematic design of a 3-DOF force-controlled end-effector module," in *Proc. IEEE 11th Conf. Ind. Electron. Appl. (ICIEA)*, Jun. 2016, pp. 1084–1089.
- [3] E. Oztemel and S. Gursev, "Literature review of industry 4.0 and related technologies," *J. Intell. Manuf.*, vol. 31, no. 1, pp. 127–182, Jan. 2020.
- [4] B. Chen, J. Wan, L. Shu, P. Li, M. Mukherjee, and B. Yin, "Smart factory of industry 4.0: Key technologies, application case, and challenges," *IEEE Access*, vol. 6, pp. 6505–6519, 2018.
- [5] Y. Kakinuma, K. Igarashi, S. Katsura, and T. Aoyama, "Development of 5-axis polishing machine capable of simultaneous trajectory, posture, and force control," *CIRP Ann.*, vol. 62, no. 1, pp. 379–382, 2013.
- [6] A. E. K. Mohammad, J. Hong, and D. Wang, "Design of a force-controlled end-effector with low-inertia effect for robotic polishing using macro-mini robot approach," *Robot. Comput.-Integr. Manuf.*, vol. 49, pp. 54–65, Feb. 2018.
- [7] S. H. Kim, E. Nam, T. I. Ha, S.-H. Hwang, J. H. Lee, S.-H. Park, and B.-K. Min, "Robotic machining: A review of recent progress," *Int. J. Precis. Eng. Manuf.*, vol. 20, no. 9, pp. 1629–1642, Sep. 2019.
- [8] C. Wu, B. Li, Y. Liu, and S. Y. Liang, "Surface roughness modeling for grinding of silicon carbide ceramics considering co-existence of brittleness and ductility," *Int. J. Mech. Sci.*, vol. 133, pp. 167–177, Nov. 2017.
- [9] J. Ning and S. Y. Liang, "Predictive modeling of machining temperatures with force–temperature correlation using cutting mechanics and constitutive relation," *Materials*, vol. 12, no. 2, p. 284, 2019.
- [10] C. Fan, J. Zhao, L. Zhang, Y. S. Wong, G. S. Hong, and W. Zhou, "Modeling and analysis of the material removal profile for free abrasive polishing with sub-aperture pad," *J. Mater. Process. Technol.*, vol. 214, no. 2, pp. 285–294, Feb. 2014.
- [11] F. Tian, C. Lv, Z. Li, and G. Liu, "Modeling and control of robotic automatic polishing for curved surfaces," *CIRP J. Manuf. Sci. Technol.*, vol. 14, pp. 55–64, Aug. 2016.
- [12] P. Xu, B. Li, C.-F. Cheung, and J.-F. Zhang, "Stiffness modeling and optimization of a 3-DOF parallel robot in a serial-parallel polishing machine," *Int. J. Precis. Eng. Manuf.*, vol. 18, no. 4, pp. 497–507, Apr. 2017.
- [13] T. Zhang, M. Xiao, Y.-B. Zou, J.-D. Xiao, and S.-Y. Chen, "Robotic curved surface tracking with a neural network for angle identification and constant force control based on reinforcement learning," *Int. J. Precis. Eng. Manuf.*, vol. 21, no. 5, pp. 869–882, May 2020.
- [14] J. Hong, A. El Khalick Mohammad, and D. Wang, "Improved design of the end-effector for macro-mini robotic polishing systems," in *Proc. 3rd Int. Conf. Mechatronics Robot. Eng. (ICMRE)*, 2017, pp. 36–41.
- [15] D. E. Whitney, "Historical perspective and state of the art in robot force control," *Int. J. Robot. Res.*, vol. 6, no. 1, pp. 3–14, Mar. 1987.
- [16] Q. Xie, H. Zhao, T. Wang, and H. Ding, "Adaptive impedance control for robotic polishing with an intelligent digital compliant grinder," in *Proc. IEEE Int. Conf. Intell. Robot. Appl. (ICIRA)*, Aug. 2019, pp. 482–494.
- [17] M. Schumacher, J. Wojtusch, P. Beckerle, and O. von Stryk, "An introductory review of active compliant control," *Robot. Auto. Syst.*, vol. 119, pp. 185–200, Sep. 2019.

- [18] L. Roveda, N. Pedrocchi, and L. M. Tosatti, "Exploiting impedance shaping approaches to overcome force overshoots in delicate interaction tasks," *Int. J. Adv. Robotic Syst.*, vol. 13, no. 5, Sep. 2016, Art. no. 172988141666277.
- [19] L. Roveda, N. Iannacci, and L. M. Tosatti, "Discrete-time formulation for optimal impact control in interaction tasks," *J. Intell. Robotic Syst.*, vol. 90, nos. 3–4, pp. 407–417, Jun. 2018.
- [20] Z. Ma, A.-N. Poo, M. H. Ang, G.-S. Hong, and H.-H. See, "Design and control of an end-effector for industrial finishing applications," *Robot. Comput.-Integr. Manuf.*, vol. 53, pp. 240–253, Oct. 2018.
- [21] G. M. Bone and M. A. Elbestawi, "Active end effector control of a low precision robot in deburring," *Robot. Comput.-Integr. Manuf.*, vol. 8, no. 2, pp. 87–96, Jan. 1991.
- [22] J. Y. Lew, "Contact control of flexible micro/macro-manipulators," in *Proc. Int. Conf. Robot. Autom.*, Apr. 1997, pp. 2850–2855.
- [23] U. A. Tol, J.-P. Clerc, and G. J. Wiens, "Micro/macro approach for dexterity enhancement of PKM's," in *Proc. Workshop Fundam. Issues Future Res. Directions Parallel Mech. Manipulators*, 2002, pp. 34–39.
- [24] L. Liao, F. Xi, and K. Liu, "Modeling and control of automated polishing/deburring process using a dual-purpose compliant toolhead," *Int. J. Mach. Tools Manuf.*, vol. 48, nos. 12–13, pp. 1454–1463, Oct. 2008.
- [25] A. S. Arifin, M. H. Ang, C. Yin Lai, and C. Wang Lim, "General framework of the force and compliant motion control for macro mini manipulator," in *Proc. IEEE/ASME Int. Conf. Adv. Intell. Mechatronics*, Jul. 2013, pp. 949–954.
- [26] T.-Y. Wu, C. Y. Lai, and S. Chen, "An adaptive neural network compensator for decoupling of dynamic effects of a macro-mini manipulator," in *Proc. IEEE Int. Conf. Adv. Intell. Mechatronics (AIM)*, Jul. 2015, pp. 1427–1432.
- [27] A. Lopes and F. Almeida, "A force-impedance controlled industrial robot using an active robotic auxiliary device," *Robot. Comput.-Integr. Manuf.*, vol. 24, no. 3, pp. 299–309, 2008.
- [28] F. Chen, H. Zhao, D. Li, L. Chen, C. Tan, and H. Ding, "Contact force control and vibration suppression in robotic polishing with a smart end effector," *Robot. Comput.-Integr. Manuf.*, vol. 57, pp. 391–403, Jun. 2019.
- [29] X. Wu, Z. Huang, Y. Wan, H. Liu, and X. Chen, "A novel force-controlled spherical polishing tool combined with self-rotation and co-rotation motion," *IEEE Access*, vol. 8, pp. 108191–108200, 2020.
- [30] G. Yang, R. Zhu, Z. Fang, C.-Y. Chen, and C. Zhang, "Kinematic design of a 2R1T robotic end-effector with flexure joints," *IEEE Access*, vol. 8, pp. 57204–57213, 2020.
- [31] L. Yuan, Z. Pan, D. Ding, S. Sun, and W. Li, "A review on chatter in robotic machining process regarding both regenerative and mode coupling mechanism," *IEEE/ASME Trans. Mechatronics*, vol. 23, no. 5, pp. 2240–2251, Oct. 2018.
- [32] H. U. Butt, D. Waleed, and R. Dhaouadi, "Friction estimation of a linear voice coil motor using robust state space sinusoidal reference tracking," in *Proc. 11th Int. Symp. Mechatronics Appl. (ISMA)*, Mar. 2018, pp. 1–6.
- [33] H. Huang, Z. M. Gong, X. Q. Chen, and L. Zhou, "Robotic grinding and polishing for turbine-vane overhaul," *J. Mater. Process. Technol.*, vol. 127, no. 2, pp. 140–145, Sep. 2002.



YISHENG GUAN (Member, IEEE) received the master's degree from the Harbin Institute of Technology, Harbin, China, in 1990, and the Ph.D. degree from Beihang University (Beijing University of Aeronautics and Astronautics, BUAA), Beijing, China, in 1998, all in mechanical engineering.

He was a Postdoctoral Fellow with the Department of Computing Science, University of Alberta, Edmonton, AB, Canada, from 1998 to 2000, and a JSPS Research Fellow with the Intelligent Systems Institute, AIST, Tsukuba, Japan, from 2003 to 2006. In 2007, he joined the School of Mechanical and Automotive Engineering, South China University of Technology, Guangzhou, China, as a Professor. Since 2013, he has been the Director of the Biomimetic and Intelligent Robotics Laboratory (BIRL) and a Professor with the School of Electromechanical Engineering, Guangdong University of Technology, Guangzhou. He has published more than 200 papers in well-known journals and at important international conferences (ten of which have won or been nominated for the Best Paper Award at the IEEE International Conference). His research interests include biomimetic robotics, intelligent robots, modular robots, and humanoids. He has chaired several IEEE international conferences (PC of ROBIO 2018 and Co-PC of ROBIO 2012 and ICIA 2009). He has been a PC member of more than 60 conferences (AE of IROS since 2012, ROBIO, AIM, ICMA, ICIA, Humanoids, and so on), and a Reviewer of about 40 international journals.



HAOWEN CHEN received the B.Eng. degree in mechanical and electronic engineering from the School of Electromechanical Engineering, Guangdong University of Technology, Guangzhou, China, in 2018. He is currently pursuing the master's degree with the Biomimetic and Intelligent Robotics Laboratory (BIRL), Guangdong University of Technology.

His main research interests include force control, robotic polishing, and intelligent manufacturing.



BING WANG received the B.Eng. degree in mechanical design, manufacturing, and automation from the School of Mechanical Engineering, University of Jinan, Jinan, China, in 2019. He is currently pursuing the master's degree with the Biomimetic and Intelligent Robotics Laboratory (BIRL), School of Electromechanical Engineering, Guangdong University of Technology, Guangzhou, China.

His main research interests include industrial robot, structure design, and motion control.



TAO ZHANG (Member, IEEE) received the B.Eng. and Ph.D. degrees from the School of Mechanical Engineering and Automation, Beihang University (Beijing University of Aeronautics and Astronautics, BUAA), Beijing, China, in 2012 and 2017, respectively.

In 2017, he joined the Biomimetic and Intelligent Robotics Laboratory, School of Electromechanical Engineering, Guangdong University of Technology, Guangzhou, China. His research interests include space robots, extraterrestrial regolith-sampling robots, seafloor regolith-sampling robots, mechanism and machine theory, mechatronic systems, and bio-inspired robotics.



JIAN LI received the M.S.E. degree in mechanical engineering from the School of Electromechanical Engineering, Guangdong University of Technology, Guangzhou, China, in 2017, where he is currently pursuing the Ph.D. degree.

His main research interests include industrial robots, smart actuator design and control, force control, robotic polishing, and intelligent manufacturing.



XINENG LIU received the M.S.E. degree from the School of Electromechanical Engineering, Guangdong University of Technology, Guangzhou, China, in 2019.

His main research interests include industrial robots, structure design, force control, robotic polishing, and intelligent manufacturing.



JIE HONG received the M.Eng. degree from the School of Electrical and Electronic Engineering, Nanyang Technological University (NTU), Singapore, in 2017. He is currently pursuing the Ph.D. degree with the College of Engineering and Computer Science, The Australian National University (ANU), Australia.

His research interests include robotics, control systems, and computer vision.



DANWEI WANG (Senior Member, IEEE) received the M.S.E. and Ph.D. degrees from the University of Michigan, Ann Arbor, MI, USA, in 1984 and 1989, respectively.

He is currently a Professor with the School of Electrical and Electronic Engineering, Nanyang Technological University (NTU), Singapore. His research interests include iterative learning control, repetitive control, fault diagnosis and failure prognosis, satellite formation dynamics and control, as well as manipulator/mobile robot dynamics, path planning, and control. He has served as an Associate Editor for the Conference Editorial Board, IEEE Control Systems Society.



HONG ZHANG (Fellow, IEEE) received the Ph.D. degree from Purdue University, West Lafayette, USA, in 1986.

He is currently a Professor with the Guangdong University of Technology, China, and the University of Alberta, Canada. His research interests include computer vision, SLAM, autonomous navigation, image processing, and robotics. He is an associate Editor of the IEEE TRANSACTIONS ON CYBERNETICS and *Robotics*.

...